

Linkage-Based Analysis and Optimization of an Underactuated Planar Manipulator for In-Hand Manipulation

Raymond R. Ma
Aaron M. Dollar

Yale University
New Haven, CT 06520

This paper investigates the in-hand manipulation capabilities of a compliant, underactuated planar robotic hand by treating the system as a simple, symmetric, 6-bar linkage mechanism with compliant joints. Although underactuated hands are generally not considered to be adept at dexterous tasks, we have found through past work that an underactuated manipulator can control n degrees of freedom with n actuators by leveraging the passive compliance to satisfy contact constraints on the object. Assuming the system to be quasi-static, the workspace of the underactuated mechanism is found through constraint-based energy minimization by sweeping through the set of allowable inputs. In this study, we investigate achievable workspaces by exploring the nondimensionalized design space, consisting of linkage ratio, joint stiffness ratio, transmission ratio, base linkage length, and object linkage length. The results of this study are useful in motivating the design of dexterous, underactuated manipulators, as well as to predict the achievable workspace of specific hand/object configurations. [DOI: 10.1115/1.4025620]

Introduction

It has been shown that underactuated robotic hands can be very proficient at grasping items of various sizes and shapes by passively adapting to the object geometry [1–3]. This adaptability allows for fewer actuators, cheaper and lighter designs, and simpler controls than fully actuated manipulators. However, since there are fewer actuators than degrees of freedom, the closing motion for each multiphalanx finger cannot be actively and fully controlled. Instead, the final hand configuration in any grasp is dependent on interactions between the fingers and the grasped object. Generally, for a hand with n actuators and m degrees of freedom, there must be $m-n$ contacts to fully constrain the hand posture.

Many underactuated hands, such as the SDM hand [3,4], utilize compliant members to obtain a statically determined system when there are fewer contacts than unconstrained degrees of freedom. These additional compliant degrees of freedom can be used to enable and facilitate dexterous, within-hand manipulation, as has been demonstrated in previous work [5,6].

This ability is largely considered to be a desirable trait for robotic hands, but its complexity for traditional rigid hands makes implementation and execution difficult, as it is synonymous with that of cooperating manipulators [7,8].

Traditional approaches to dexterous, in-hand manipulation [9] suggest a minimum of three fingers with three degrees of freedom each in order to fully constrain an object while moving it within SE(3). Many robotic hands still utilize this topology. In the general case, $n+1$ actuators are required to constrain and manipulate an object with n degrees of freedom [10], where one actuator is dedicated to fixing the object to the manipulator (i.e., generating an internal constraint force on the object). However, springs can be used in place of one or more of these “actuators,” albeit at the

cost of active control. With proper attention to the design of the hand, passively driven joints such as these can be effectively used to simplify the hand structure and control without sacrificing significant performance.

In this paper, we build on the work from Ref. [5] and treat the underactuated manipulation problem as a conservative system, where the passive compliance in the elastic finger joints serves to help constrain the object. The system model is then simplified as an underactuated parallel 6-bar mechanism with preloaded, compliant joints, and the object is treated as the link between two 2-DOF underactuated fingers (Fig. 1). We determine the workspace of such systems by energy minimization [11] and utilize it to motivate future hand designs optimized for dexterity.

Representing in-hand manipulation as a closed kinematic chain is not a novel concept. Williams [8] and Montana [12] discuss the “virtual linkage” explicitly in describing cooperative manipulation, modeling grasped objects as a mechanism with actuated joints characterizing the internal forces. Bicchi et al. have established a framework for describing the manipulability and mobility of multiple limb robots [7,13,14] as general closed-chain mechanisms. Likewise, the kinematic workspace of planar, closed-loop mechanisms is a well-studied topic [15–19], but those analyses do not account for the underactuation and passive compliance detailed in this work.

The authors are unaware of any work in which such models have been used in order to optimize the design of dexterous hands or in combination with underactuated fingers. We begin the paper with the presentation of the analysis model describing this system.

Analytic Framework

Our analysis focuses on the SDM hand’s compliant fingers, modeled as two-link revolute–revolute fingers with single-acting cable-driven system and elastic compliance at each joint. Tendon position control, as opposed to tendon force control, is used to actuate each finger. As shown in Fig. 1, each finger is comprised of a proximal pin joint preloaded by an extension spring, and a

Contributed by the Mechanisms and Robotics Committee of ASME for publication in the JOURNAL OF MECHANISMS AND ROBOTICS. Manuscript received August 1, 2012; final manuscript received August 21, 2013; published online November 6, 2013. Assoc. Editor: Qiaode Jeffrey Ge.

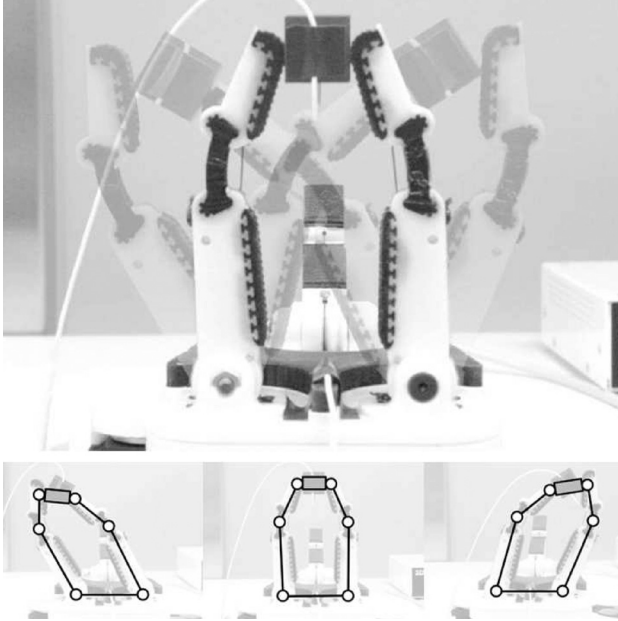


Fig. 1 Underactuated SDM hand motivating this study on dexterity

distal flexure joint. A pseudorigid body model is shown in Fig. 2. Detailed in Refs. [20,21], these fingers have the following constraints:

$$C_{aa} = 0 = r_a \Delta \theta_a - J_a \Delta \vec{\theta} \quad (1)$$

$$U_{\text{Finger}} = \frac{1}{2} \Delta \vec{\theta}^T K \Delta \vec{\theta} \quad (2)$$

$$-K \Delta \vec{\theta} + J_C^T f_e + J_a^T f_a = 0 \quad (3)$$

$$\Delta \vec{\theta} = \begin{bmatrix} \Delta \theta_P \\ \Delta \theta_D \end{bmatrix} \quad (4)$$

$$K = \begin{bmatrix} k_P & 0 \\ 0 & k_D \end{bmatrix} \quad (5)$$

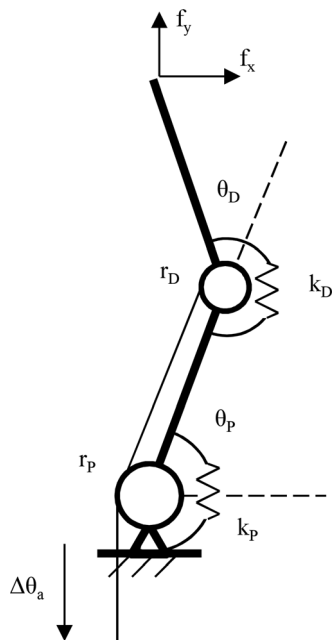


Fig. 2 Basic pseudorigid body model for the SDM finger

$$J_C = \begin{bmatrix} -L_P \sin \theta_P - L_D \sin(\theta_P + \theta_D) & -L_D \sin(\theta_P + \theta_D) \\ L_P \cos \theta_P + L_D \cos(\theta_P + \theta_D) & L_D \cos(\theta_P + \theta_D) \end{bmatrix} \quad (6)$$

$$J_a = [r_P \quad r_D] \quad (7)$$

$$f_e = J_C^{-T} [K \Delta \theta - J_a^T f_a] \quad (8)$$

In determining workspace, this study assumes that the required tendon force f_a for a given actuation $\Delta \theta_a$ can always be generated. For simplicity in this text, we set the actuation pulley radius equal to 1 so that the actuated tendon length displacement is also $\Delta \theta_a$. In the absence of external disturbances, where endpoint force $f_e = [0 \ 0]^T$, the unloaded finger configuration can be found through energy minimization or force balance

$$\Delta \theta'_D = \frac{k_P r_D \Delta \theta_a}{k_D r_P^2 + k_P r_D^2} \quad (9)$$

$$\Delta \theta'_P = \frac{\Delta \theta_a - r_D \Delta \theta'_D}{r_P} \quad (10)$$

$$f'_a = \frac{k_D \Delta \theta'_D}{r_D} = \frac{k_P \Delta \theta'_P}{r_P} \quad (11)$$

The restorative nature of the compliant joints ensures that the underactuated finger will attempt to restore to this unloaded configuration. Due to the kinematic actuation constraint in Eq. (1), the joints will deviate in opposite directions when the fingertip is perturbed for a constant $\Delta \theta_a$ actuation.

For a fixed actuation input $\Delta \theta_a$ in position control, adjusting the tendon force affects both the output force magnitude and direction. The tendon force must be greater than or equal to the tendon force f'_a necessary to drive the finger to the unloaded finger configuration described in relations (9)–(11). The force at the tip determines the final configuration of the finger. Figure 3 shows that by driving the fingers past the point of contact on the object, the fingers now impart a reacting force on the object as the system tries to restore the unloaded configuration. If a configuration exists where the object remains in contact with the fingertips, then the system as a whole can be treated as a closed-chain mechanism, where a linkage of length L_O represents the grasped object. The lowest energy solution satisfying the constraints for such an elastic system is the final stable grasping pose [11,22].

Pinch grasping and precision manipulation with underactuated fingers are frequently characterized in literature by analyses of force capability of individual fingers [23–26]. These studies treat pinch-grasping as a subset of power-grasping, focusing on only the normal forces applied by the phalanges. In order to satisfy the

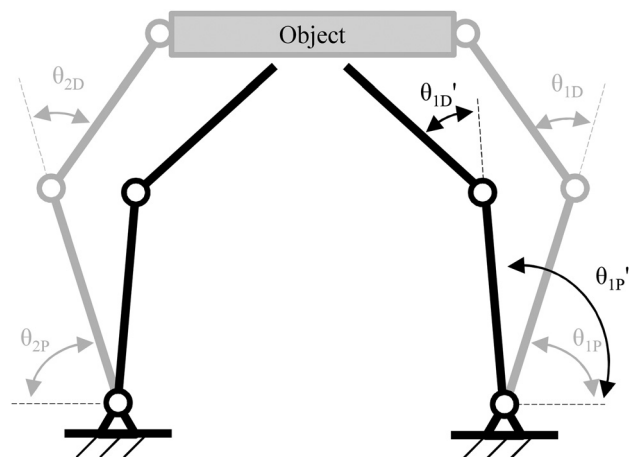


Fig. 3 When an object deflects the SDM finger from its unloaded configuration, passive compliance from the loaded joints can apply a closing force on the object

constraints put forth in these models, the distal phalanges of these idealized fingers must remain parallel to one another. Although hands such as the SARAH hand [27], and even previous implementations of the SDM hand [28], have mechanical designs to accommodate that pinch configuration, this constraint limits the workspace of the hand system as a whole and does not properly reflect real-world systems.

We have shown empirically through past experiments [5,6] that stable precision grasping is achievable with the hand shown in Fig. 1 without maintaining the distal phalanges at parallel. This study relaxes the constraints of the underactuated precision manipulation model in order to obtain a more broad view of the in-hand manipulation problem, independent of strict contact constraints. In this study, the model assumes frictionless, no-slip point contacts. In stable, minimal energy configurations, the system behaves like a 6-bar linkage mechanism with pin-joints.

While object geometry and type of fingertip contact have significant impact on the stability of pinch grasps, this study seeks to focus on the impact of other design parameters on the achievable workspace.

Kinematic Analysis

Figure 4 shows the kinematic closed-chain representation of the planar two-finger manipulation system. The object is described by a linkage of length L_O with center-point $P(x, y, \theta_0)$, denoting the position and orientation of the object linkage with respect to the global reference frame O . The system is symmetric, with the finger-bases separated by $2L_B$. In analyzing the kinematic workspace, this study utilizes a normalized design space where: $L_P + L_D = 1$. The L_O and L_B values are then nondimensionalized with respect to the total finger length. Relevant work [25] suggests an average palm to finger, $2L_B$ to $(L_P + L_D)$ ratio of 0.56.

The kinematic chain must satisfy the following constraints:

$$x_1 = L_B + L_{1P} \cos(\theta_{1P}) + L_{1D} \cos(\theta_{1P} + \theta_{1D}) \quad (12)$$

$$y_1 = L_{1P} \sin(\theta_{1P}) + L_{1D} \sin(\theta_{1P} + \theta_{1D}) \quad (13)$$

$$x_2 = -L_B - L_{2P} \cos(\pi - \theta_{2P}) - L_{2D} \cos(\pi - \theta_{2P} - \theta_{2D}) \quad (14)$$

$$y_2 = L_{2P} \sin(\pi - \theta_{2P}) + L_{2D} \sin(\pi - \theta_{2P} - \theta_{2D}) \quad (15)$$

$$C_{kk} = 0 = (x_1 - x_2)^2 + (y_1 - y_2)^2 - L_o^2 \quad (16)$$

The inverse kinematics (IK) for the fully actuated chain has four branches, since the IK solution for each finger has two solutions. However, for the underactuated case, where the joint stiffness determines the force balance on the object linkage, there is only a single solution branch to consider for IK.

The maximal manipulation workspace is traditionally found by finding the intersection of the workspaces of the individual legs/

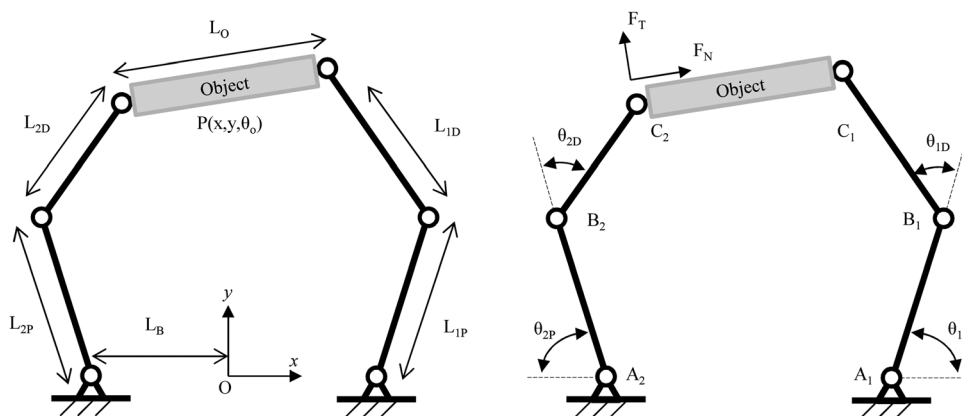


Fig. 4 Closed kinematic chain representation of the planar manipulation problem. Assuming contact constraints hold, the system can be viewed as a 6-bar linkage.

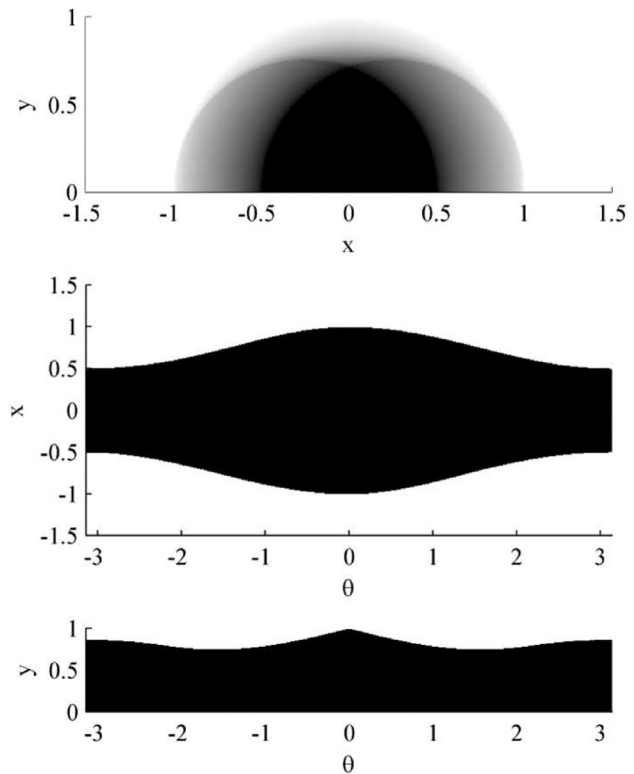


Fig. 5 Sample kinematic workspace for linkage with parameters $L_P = L_D = 0.5$, $L_B = 0.25$, $L_O = 0.5$. Greater intensity in top-most plot indicates more achievable orientations at that x - y location

fingers [15,29,30], assuming the individual digits are fully actuated. The workspaces and manipulability of similar parallel mechanisms have been thoroughly discussed in literature. In this study, a planar Cartesian region (x, y, θ) bounded by $[-1.5, 1.5]$, $[0.0, 1.0]$, and $[-\pi, \pi]$, respectively, is discretized, and each point is sampled and checked against the specified kinematic constraints (12)–(16). Workspace coverage is defined as the proportion of this region that the closed-chain mechanism can reach. Figure 5 shows an example workspace with sample linkage configurations overlaid on top. Because a fully actuated 6-bar mechanism is redundantly defined by four joints, there may be multiple achievable orientations for each point in Cartesian xy space. This is not the case for the underactuated manipulation model in this study, which only has two actuators.

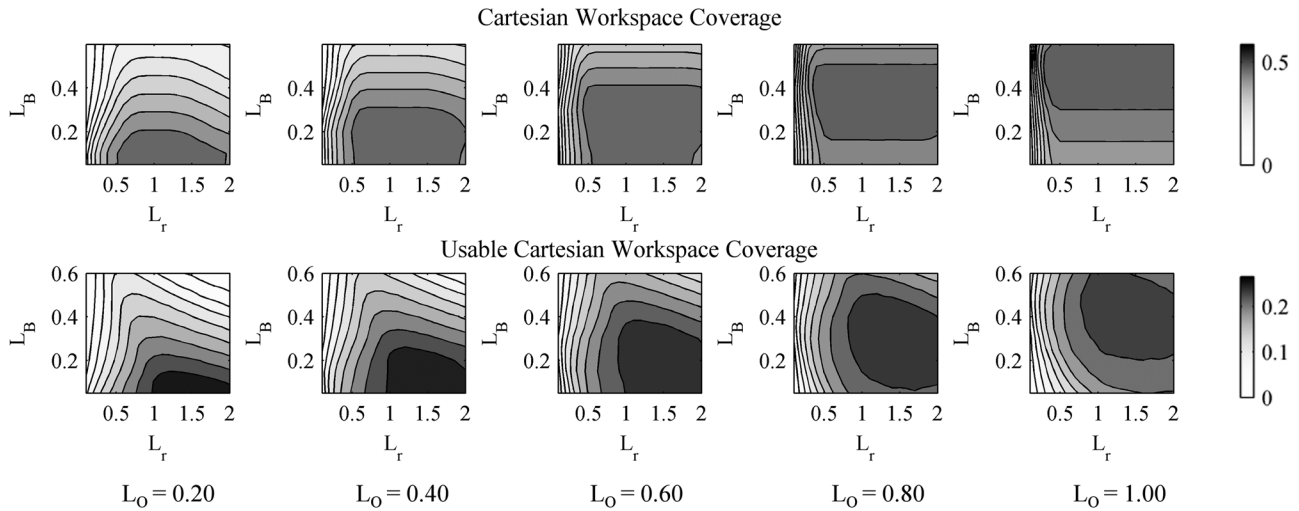


Fig. 6 Cartesian kinematic workspace coverage for varying L_r , L_B , L_O parameter values. Higher intensity indicates that parameter combination results in greater coverage of the workspace.

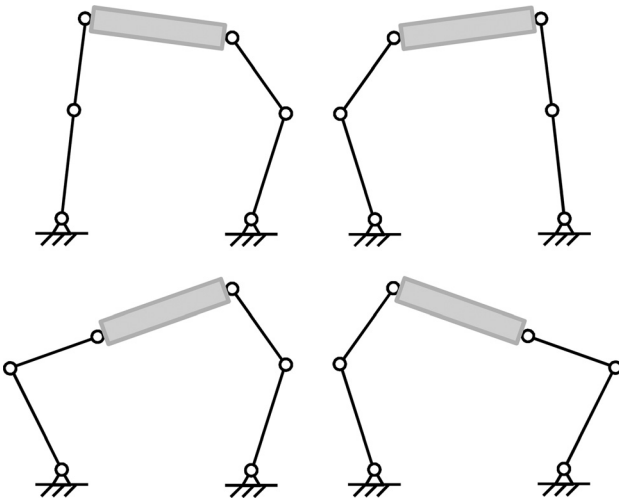


Fig. 7 Stationary singularities for the 6-bar closed chain. Setting bounds on the actuation constraints ensure that underactuated manipulator never reach these unstable configurations.

As shown in the top plot of Fig. 6, the optimal linkage ratio for complete kinematic Cartesian workspaces is $L_r = 1$, as calculated by previous research [14]. However, for a hand with an L_B value of 0.25, the analysis suggests linkage ratio $L_r = 1.3$ to maximize the Cartesian workspace. Figure 6 also shows that workspace improves as the ratio $L_O/(2L_B)$ approaches unity for small values of L_O and L_B . To accommodate power-grasping, values of L_B should be in the range [0.2, 0.3], which reduces the in-hand manipulability of the hand. This relation provides some additional evidence that dexterity and power-grasping are fundamentally different tasks with opposing requirements.

The singularities of the kinematic chain can be found and classified by differentiating the constraint equations (12)–(16) and considering the velocity equations of the form

$$J_{\text{parallel}} = A^{-1}B \quad (17)$$

$$A\dot{\theta} = B\dot{p} \quad (18)$$

This formulation separates the singularities of the system into three different categories [15,31]. The *stationary singularity* occurs when A is singular but B is not. These singularities account

for the mechanism at the boundaries of its workspace; for example when $\theta_D = 0$. The *uncertainty singularity*, where B is singular but A remains invertible, accounts for configurations where the closed kinematic chain loses a degree of freedom. This occurs when a joint becomes coincident with another in the system. This singularity and the final singularity type, where both A and B are singular, are generally not problematic singularities that we have to consider in practical applications.

Liu [15] defines the *usable workspace* as the maximum portion of the theoretical workspace which is devoid of any singularities and bound by the loci of the system singularities. In precision manipulation, especially with underactuated fingers, it has also been shown that maintaining a pinch grasp on an object outside of this usable workspace has not been achievable [6] due to the poses' susceptibility to ejection. Figure 7 denotes the stationary singularities that the 6-bar underactuated chain may undergo. In practice, we do not need to consider uncertainty singularities. Because an underactuated closed chain resolves to the lowest energy configuration, there is also no need to consider the alternative IK solution for each finger. To calculate the usable workspace of the underactuated system and avoid stationary singularities, the following joint constraints were also applied

$$\theta_{1D} > 0, \quad \theta_{2D} > 0 \quad (19)$$

$$\pi - (\theta_{2P} + \theta_{2D}) > \theta_0 \quad (20)$$

$$\pi - (\theta_{1P} + \theta_{1D}) > -\theta_0 \quad (21)$$

Figure 8 shows sample workspaces for three different finger length ratios, as well as the difference between the full kinematic workspace and usable workspace, bound by the finger linkage singularities. For practical purposes, the usable workspace provides more insight than the full theoretical workspace, as control methodologies should seek to avoid singular configurations or transitions that move through singular configurations. For the underactuated 6-bar mechanism, assuming the resting joint positions are not less than 0, each finger would only move through stationary singularities if buckling were to occur. However, given the actuation constraint (1), buckling is unlikely, and the new finger configuration would correspond to a different actuation input $\Delta\theta_a$.

Referring back to Fig. 6, a selection of linkage ratio L_r greater than 1, in the range [1.2, 1.7], is desired to optimize the usable workspace. The SDM hand fingers [5], as well as fingers for other underactuated hands [25], utilize a linkage ratio $L_r = 1.5$, a closer approximation to the phalanx ratio inherent in human hands.

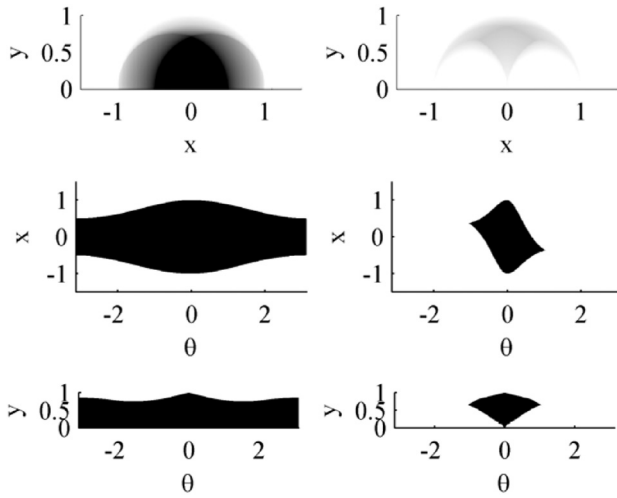


Fig. 8 Comparison of full (left) versus usable (right) kinematic workspaces for parameters $L_P = L_D = 0.5$, $L_B = 0.25$, $L_O = 0.5$. As in Fig. 5, top-most Cartesian workspace has higher intensity at x - y locations with greater degree of achievable orientation.

Underactuated Closed-Chain

The workspace of the underactuated chain is determined by finding the system configuration with lowest energy satisfying the kinematic constraints (12)–(16) and actuation constraint (1) for the range of all feasible actuation inputs $\Delta\theta_a$ for each finger. The model presented here assumes no gravity and quasi-static behavior, consistent with the authors' previous experimental work [6].

An additional force constraint is added to ensure that there is only compressive force acting on the object linkage, and that the tendon force is applied such that the force is directed through the object (f_c is a scaling constant)

$$f_c = \begin{bmatrix} f_x \\ f_y \end{bmatrix} = \begin{bmatrix} 1 \\ \tan \theta_o \end{bmatrix} f_c = \vec{b} f_c \quad (22)$$

$$0 = -K\Delta\theta + J_c^T \vec{b} f_c + J_a^T f_a \quad (23)$$

$$\begin{bmatrix} f_c \\ f_a \end{bmatrix} = [J_c^T \vec{b} \quad J_a^T]^{-1} K\Delta\theta \quad (24)$$

The elastic energy function of the system to be minimized is

$$U = \sum_{i=1}^4 \frac{1}{2} k_i (\theta_i - \theta_{i0})^2 \quad (25)$$

The SDM fingers have single-acting tendon actuation systems, which can only apply force in one direction. To avoid cases where the tendon may go slack, this model also requires that the tendon force for a given energy-minimal solution be greater than the tendon force required for that finger's unloaded configuration, from relation (11). The actuation force and usable workspace (19)–(21) constraints were applied after energy minimization was performed on the system (25) with the previously specified kinematic constraints (1) and (16).

This model does not attempt to account for the ability of underactuated fingers to acquire stable pinch grasps on any particular object geometries or materials. Figure 1 affirms that in practice, the geometry of the object and the fingertips play a significant role in determining the achievable in-hand workspace and object trajectory. The lowest energy configuration does not necessarily guarantee a stable grasp satisfying all frictional constraints for a given pair of actuation inputs, but the resulting workspace gives insight regarding the subsets of the actuation space where a pinch grasp may be most stable.

Table 1 Nomenclature

Parameter	Definition
r_P, r_D	Transmission pulley radius (proximal, distal)
r_a	Actuation pulley radius (set to 1 for simplicity)
R_r	Transmission ratio (r_P/r_D)
k_P, k_D	Joint stiffness
K_r	Joint stiffness ratio (k_P/k_D)
L_P, L_D	Linkage lengths
L_B	Half the distance between finger bases
L_O	Object linkage length
L_r	Linkage ratio (L_P/L_D)
$\Delta\theta_a$	Actuation displacement
$r_a\Delta\theta_a$	Tendon length displacement
$\Delta\theta_P, \Delta\theta_D$	Joint displacement from rest position
θ_P, θ_D	Joint position
θ_{P0}, θ_{D0}	Rest joint position
f_a	Tendon force
f_c	Finger endpoint output force

Justification for this simplified model comes primarily from empirical results [5,6,28], where two-link fingers with minor modifications, namely, soft, rounded fingertips, show this linkage-based behavior. Compliance of an additional third distal joint can be added and designed to optimally maintain a parallel configuration, an option that will be investigated in future work.

In addition to linkage length selections, the design space for the underactuated model also includes the transmission ratio R_r , joint stiffness ratio K_r , and resting joint positions. Ratios were normalized such that $r_P + r_D = 1$ and $k_P + k_D = 1$, although there did not need to be restrictions on the scaling of those parameters (Table 1).

Optimization of relation (25) under the kinematic closed-chain constraint (16) and the actuation constraints (1) for each finger can be performed with application of Lagrange Multipliers and available numerical constraint solvers. However, given the size and dimensionality of the parameter search, the authors found that an exhaustive, brute-force search of a discretized workspace was a much more tractable and efficient approach.

The discretized workspaces for a total of 102,400 parameter combinations were computed for this study. Running on four computing nodes (each with 2.83 Xeon CPU cores and 16 GB ram running eight parallel threads), this optimization took 12 h to complete. The design space bounds for linkage ratio L_r , object length L_O , base length L_B , transmission ratio R_r , and stiffness ratio K_r were [0.1, 2.0], [0.1, 1.0], [0.1, 0.5], [0.25, 2.0], and [0.25, 2.0], respectively. These value ranges were chosen to encompass the common design ranges in existing robotic hands.

Results and Analysis

Figure 9 shows sample workspaces for a variety of parameter selections for a given object linkage length L_O . Unlike the kinematic workspaces, achievable orientations are coupled with points in the Cartesian workspace. Designers should consider the areas in the workspace where the ability to change orientations is more desirable. Due to underactuation, orientation and Cartesian position cannot be adjusted independently.

Figure 10 analyzes the effect of the selection of resting joint values on the achievable workspaces. Although increasing the resting joint may limit the power-grasping capabilities of a manipulator with single-acting fingers, doing so at the proximal joint improves the achievable workspace while shifting the optimal linkage ratio L_r to a more anthropomorphic range.

For all sampled workspaces, the achievable orientations are most limited along the outer edge of the workspace and along the middle axis. In practice, underactuated manipulators can only initiate pinch grasps on objects along the upper boundary of these workspaces, where fingertip forces are the smallest [6]. Underactuation in this system implies that each finger cannot independently control position and force output, so the force exerted on the

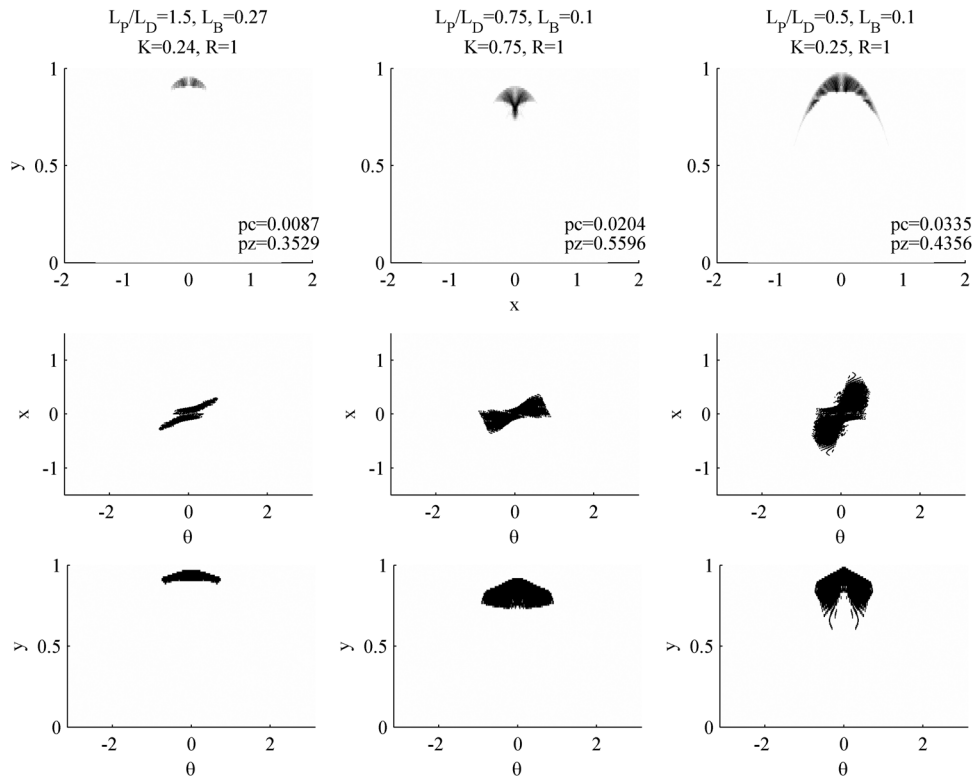


Fig. 9 Underactuated workspaces for object length $L_O = 0.2$. First column utilizes parameter values from exemplar SDM hand. Second column utilizes parameters from configuration optimal in orientation. Third column utilizes parameters from configuration optimal in Cartesian workspace. Proportion of coverage in Cartesian xy space is denoted by pc , coverage in orientation is denoted by pz .

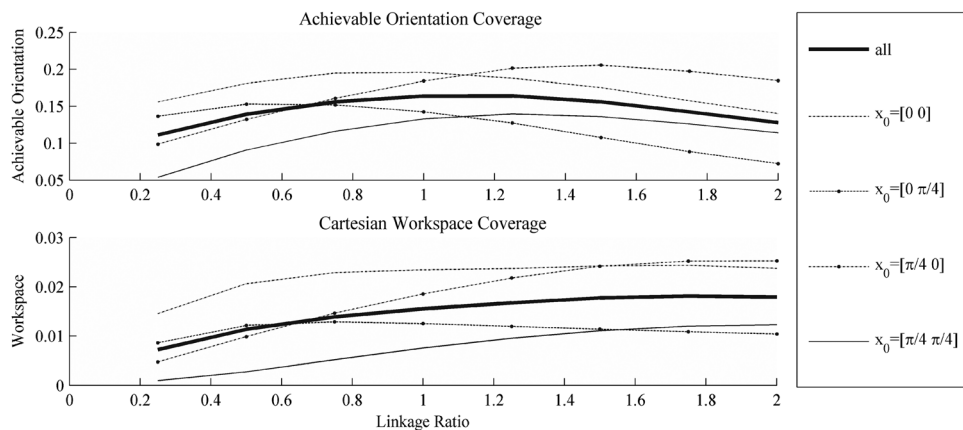


Fig. 10 Workspaces for underactuated manipulation linkage with respect to linkage ratio for a selection of initial joint positions

object linkage depends on the energy-minimal configuration of the hand. As the object is pulled in further into the workspace, the number of achievable orientations increases, as does the force exerted by the fingertips and the possibility of instability and object ejection. The workspace region along the middle axis with the largest variation in orientation may be unobtainable in practice due to the increase in forces. Figure 11 illustrates this characteristic of underactuated pinch grasps in more detail.

Figures 12 and 13 detail the optimal design choices for the remaining parameters. Each parameter set's orientation metric is defined as the proportion of unique orientations the object linkage can reach over a discretized orientation range $[-\pi/2, \pi/2]$. For

both orientation and Cartesian space, these simulations favor a linkage ratio L_r in the range [1.0, 1.6], a transmission ratio R_r of approximately 1, and low stiffness ratios K_r less than 1. This correlates favorably with the parameter values with which we have found success in recent experiments [5,6]. For comparison, the SDM hand has linkage ratio $L_r = 1.5$, base length $L_B = 0.27$, transmission ratio $R_r = 1.0$, stiffness ratio $K_r = 0.24$, and resting joint positions at [0.0, 0.0].

Design configurations with low linkage ratios and high stiffness ratios produced the smallest workspaces in Cartesian space and achievable orientation. Relations (9)–(11) indicate that such configurations would act like hands with rigid, single-degree-of-

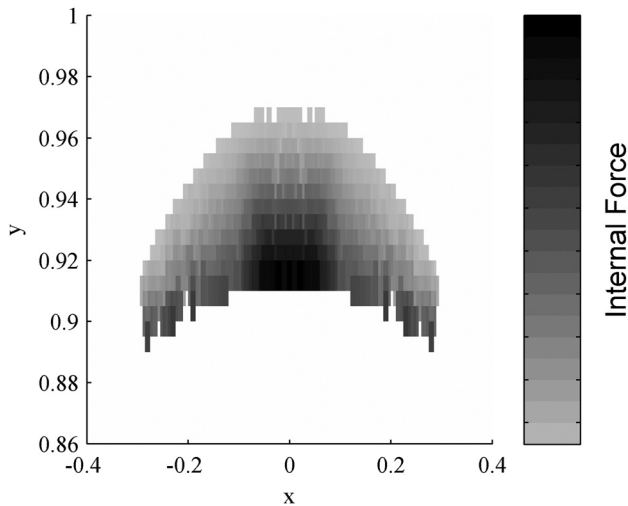


Fig. 11 Close-up of Cartesian workspace from Fig. 9, where $L_P/L_D = 1.5$, $L_B = 0.27$, $K = 0.24$, $R = 1$, showing how internal force on the object linkage varies according to position. Internal force is normalized with respect to the maximum internal force measured for this workspace.

freedom, single-link fingers. The resulting workspaces are isolated to a thin arc along the upper boundary of the corresponding maximal kinematic workspace. Higher linkage ratios and smaller stiffness ratios lead to better performance by shifting compliance toward the point of contact with the object and allowing each finger to adjust more to accommodate the object and opposing finger.

The results shown in Figs. 12 and 13 account for all object lengths in the range $[0.1, 1.0]$, but similar trends were seen when the dataset was divided in small ($L_O < 0.5$) and large ($L_O > 0.5$) objects.

Limitations and Future Work

It was not the intent of this study to accurately predict the dexterity or workspaces of underactuated finger-based manipulators. Rather, this was an attempt to establish a set of guidelines for intelligently selecting design parameters in future experimental studies on manipulation with underactuated fingers.

By utilizing a model that assumes such simplifications, we establish an upper bound on the possible workspace, prioritizing parameters over which designers have complete control (i.e., linkage lengths, stiffness, transmission) instead of characteristics that can vary greatly between tasks (i.e., contact conditions). To that

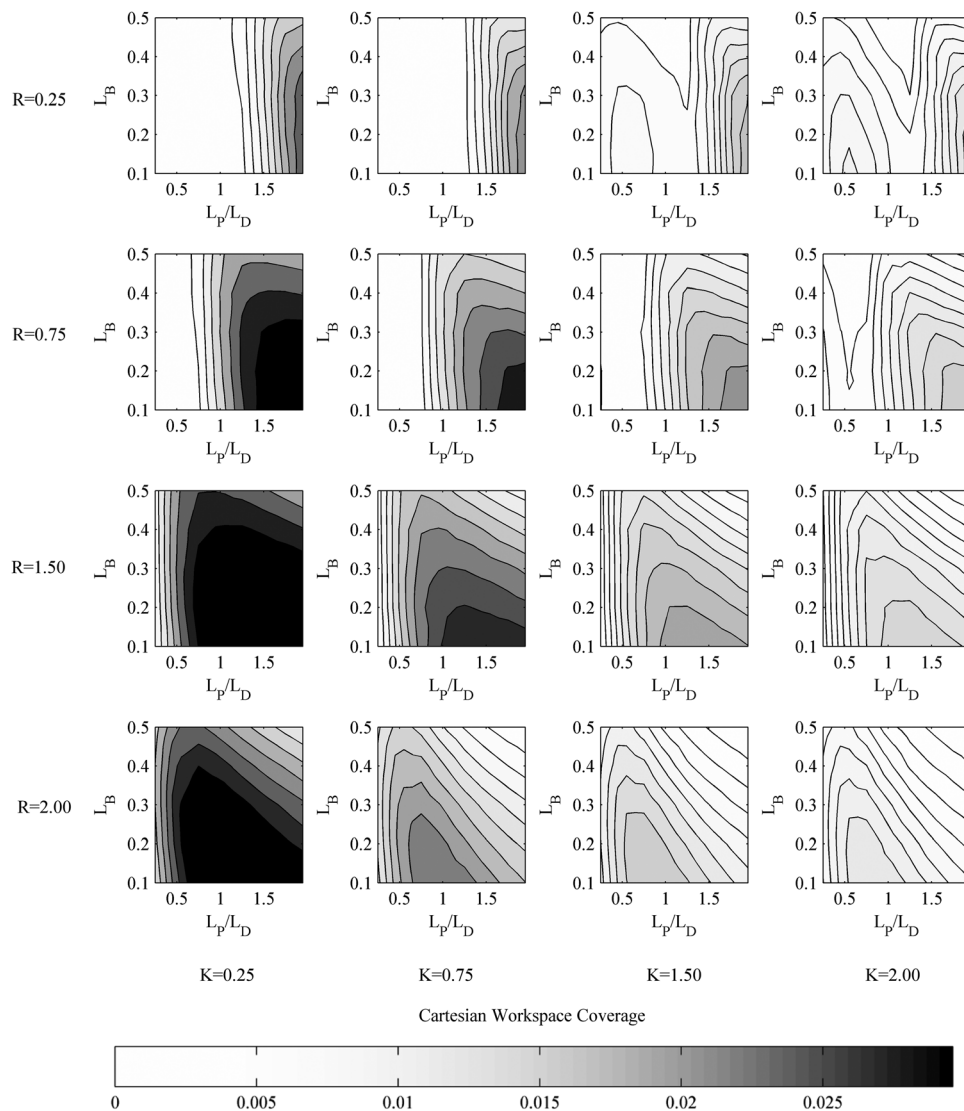


Fig. 12 Contour plots detailing the reachable calculated Cartesian workspaces for the range of system parameters, averaged over all object sizes

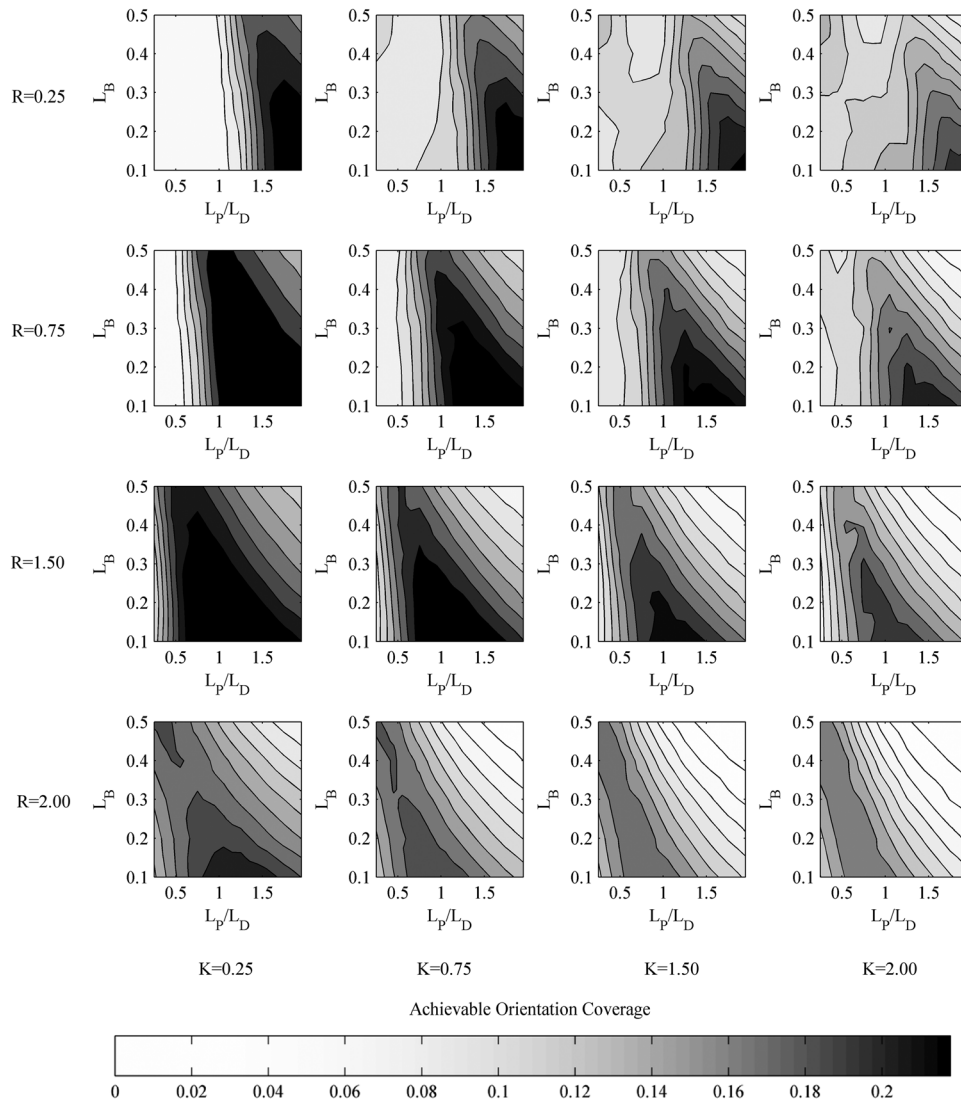


Fig. 13 Contour plots detailing the calculated achievable orientations for the range of system parameters, averaged over all object sizes

effect, results from this study are in accord with the design parameters used in existing implementations of underactuated manipulators, previously found through extensive trial and error.

While this model assumes a symmetric hand, asymmetry in-hand design may lead to more interesting results, especially with respect to control. Consider the planar dexterity of the human thumb and index finger, arguably the two fingers primarily responsible for dexterity in the anthropomorphic hand: if we approximate the distal and mid phalanges of the index finger as a single phalanx, the corresponding linkage ratio is nearly 1, whereas the linkage ratio for the two thumb phalanges is 1.37 [32]. Researchers have previously discussed decoupling the force and position control in cooperative manipulation [33] through dedicated pusher and steerer components. The parameters of underactuated manipulators can be chosen to inherently satisfy these distinct roles.

Other work [29] also suggests the notion of a home configuration, the point in Cartesian space where the maximum number of orientations θ can be reached. The nonhomogeneity of underactuated workspaces suggests this may be a point of interest. There may be a corresponding configuration in underactuated hand systems denoting the optimal initial precision grasp prior to manipulation. We will seek to investigate these areas further through experimental studies in future work.

Conclusion

In this paper, the workspace of an underactuated, symmetric 6-bar parallel mechanism with compliant joints is analyzed. The system models the underactuated in-hand manipulation problem by simplifying the contact conditions. The usable workspace of the mechanism can be found through energy minimization on the set of solutions satisfying the kinematic and actuation constraints.

The optimal system parameters for the usable workspace of the underactuated system deviate from those of the purely kinematic system. The notion of a usable workspace, bounded by the stationary singularities of the system, can be more useful in describing the practical capabilities of these manipulator models. The design parameters can be selected to prioritize either coverage in Cartesian xy space or object rotation capability. Designers should be careful to not only consider the overall size of achievable workspace, but also the distribution of orientation capability within each workspace.

Acknowledgment

The authors would like to thank Lael Odhner and Joe Belter for helpful discussion on this topic.

References

- [1] Hirose, S., and Umetani, Y., 1978, "The Development of Soft Gripper for the Versatile Robot Hand," *Mech. Mach. Theory*, **13**, pp. 351–359.
- [2] Birglen, L., Gosselin, C., and Laliberte, T., 2008, "Underactuated Robotic Hands," Vol. 40., *Springer Tracts in Advanced Robotics*, p. 13.
- [3] Dollar, A. M., and Howe, R.D., 2010, "The Highly Adaptive SDM Hand: Design and Performance Evaluation," *Int. J. Rob. Res.*, **29**(5), pp. 585–597.
- [4] Dollar, A., and Howe, R., 2011, "Joint Coupling Design of Underactuated Hands for Unstructured Environments," *Int. J. Rob. Res.*, **30**(9), pp. 1157–1169.
- [5] Odhner, L., Ma, R., and Dollar, A., 2012, "Precision Grasping and Manipulation of Small Objects From Flat Surfaces Using Underactuated Fingers," Proceedings of IEEE International Conference on Robotics and Automation, pp. 2830–2835.
- [6] Odhner, L., Ma, R., and Dollar, A.M., 2012, "Experiments in Underactuated In-Hand Manipulation," Proceedings of 13th International Symposium on Experimental Robotics (ISER).
- [7] Bicchi, A., Melchiorri, C., and Balluchi, D., 1995, "On the Mobility and Manipulability of General Multiple Limb Robots," *IEEE Trans. Rob. Autom.*, **11**(2), pp. 215–228.
- [8] Williams, D., and Khatib, O., 1993, "The Virtual Linkage: A Model for Internal Forces in Multi-Grasp Manipulation," Proceedings of International Conference on Robotics and Automation, pp. 1025–1030.
- [9] Salisbury, J., and Craig, J., 1982, "Articulated Hands: Force Control and Kinematic Issues," *Int. J. Rob. Res.*, **1**(1), pp. 4–17.
- [10] Mason, M.T., and Salisbury, J., 1985, *Robot Hands and the Mechanics of Manipulation*, MIT Press, Cambridge, MA.
- [11] Hanafusa, H., and Haruhiko, A., 1977, "Stable Prehension by a Robot Hand With Elastic Fingers," Proceedings of 7th International Symposium Industrial Robots.
- [12] Montana, D., 1995, "The Kinematics of Multi-Fingered Manipulation," *IEEE Trans. Rob. Autom.*, **11**(4), pp. 491–503.
- [13] Bicchi, A., and Prattichizzo, D., 2000, "Manipulability of Cooperating Robots With Unactuated Joints and Closed-Chain Mechanisms," *IEEE Trans. Rob. Autom.*, **16**(4), pp. 336–345.
- [14] Yoshikawa, T., 1985, "Manipulability of Robotic Mechanisms," *Int. J. Rob. Res.*, **4**(3), pp. 3–9.
- [15] Liu, X., Wang, J., and Pritschow, G., 2006, "Kinematics, Singularity and Workspace of Planar 5R Symmetrical Parallel Mechanisms," *Mech. Mach. Theory*, **41**, pp. 145–169.
- [16] Gosselin, C., and Jorge, A., 1990, "Singularity Analysis of Closed-Loop Kinematic Chains," *IEEE Trans. Rob. Autom.*, **6**(3), pp. 281–290.
- [17] Merlet, J.-P., Clement, M. G., and Nicolas, M., 1998, "Workspaces of Planar Parallel Manipulators," *Mech. Mach. Theory*, **33**(1), pp. 7–20.
- [18] Park, F. C., and Jin, W. K., 1999, "Singularity Analysis of Closed Kinematic Chains," *ASME J. Mech. Des.*, **121**, pp. 32–38.
- [19] Borras, J., and Dollar, A. M., 2013, "A Parallel Robots Framework to Study Precision Grasping and Dexterous Manipulation," Proceedings of International Conference on Robotics and Automation, Karlsruhe, Germany, May 6–10.
- [20] Balasubramanian, R., Belter, J., and Dollar, A., 2010, "External Disturbances and Coupling Mechanisms in Underactuated Hands," Proceedings of IDETC, Montreal, Quebec.
- [21] Balasubramanian, R., and Dollar, A., 2011, "Variation in Compliance in Two Classes of Two-Link Underactuated Mechanisms," Proceedings of International Conference on Robotics and Automation, pp. 3497–3504.
- [22] Vukobratovic, M., and Tuneski, A., 1998, "Mathematical Model of Multiple Manipulators: Cooperative Compliant Manipulation on Dynamical Environments," *Mech. Mach. Theory*, **33**, pp. 1211–1239.
- [23] Kragten, G. A., Baril, M., Gosselin, C., and Herder, J., 2011, "Stable Precision Grasps by Underactuated Grippers," *IEEE Trans. Rob.*, **27**(6), pp. 1056–1066.
- [24] Kragten, G., and Herder, J., 2010, "The Ability of Underactuated Hands to Grasp and Hold Objects," *Mech. Mach. Theory*, **45**(3), pp. 408–425.
- [25] Laliberte, T., and Gosselin, C., 1998, "Simulation and Design of Underactuated Mechanical Hands," *Mech. Mach. Theory*, **33**(1-2), pp. 39–57.
- [26] Birglen, L., and Gosselin, C., 2004, "Kinestatic Analysis of Underactuated Fingers," *IEEE Trans. Rob. Autom.*, **20**(2), pp. 211–221.
- [27] Rubinger, B., et al, 2001, "Self-Adapting Robotic Auxiliary Hand (SARAH) for SPDM Operations on the International Space Station," Proceedings of I-SAIRAS, Quebec, Canada.
- [28] Odhner, L., and Dollar, A., 2011, "Dexterous Manipulation With Underactuated Elastic Hands," Proceedings of International Conference on Robotics and Automation, pp. 5254–5260.
- [29] Gosselin, C., and Angeles, J., 1988, "The Optimum Kinematic Design of a Planar Three-Degree-of-Freedom Parallel Manipulator," *ASME J. Mech. Trans. Autom. Des.*, **110**(1), pp. 35–41.
- [30] Kumar, V., and Gardner, J., 1990, "Kinematics of Redundantly Actuated Closed Chains," *IEEE Trans. Rob. Autom.*, **6**(2), pp. 269–274.
- [31] Gosselin, C., and Angeles, J., 1990, "Singularity Analysis of Closed-Loop Kinematic Chains," *IEEE Trans. Rob. Autom.*, **6**(3), pp. 281–290.
- [32] Pozanski, A., 1974, *The Hand in Radiologic Diagnosis*, W. B. Saunders Company, Philadelphia, PA.
- [33] Brown, R., and Jennings, J., 1995, "Manipulation by a Pusher/Steerer," Proceedings of Intelligent Robot Systems, Pittsburgh, PA.